Available online at www.sciencedirect.com
SCIENCE DIRECT
Polymer 46 (2005) 2472–2485
polymer
www.elsevier.com/locate/polymer

Polyelectrolyte-functionalized multiwalled carbon nanotubes: preparation, characterization and layer-by-layer self-assembly

Hao Kong[a], Ping Luo[a], Chao Gao[a,b,*], Deyue Yan[a]

[a]College of Chemistry and Chemical Engineering, Shanghai Jiao Tong University, 800 Dongchuan Road, Shanghai 200240, P. R. China
[b]Sussex Nanoscience and Nanotechnology Centre (SNNC), Department of Chemistry, School of Life Sciences, University of Sussex, Brighton BN1 9QJ, UK

Received 1 November 2004; received in revised form 21 January 2005; accepted 23 January 2005

Abstract

Two kinds of polyelectrolyte: polyacrylic acid (PAA) and poly(sodium 4-styrenesulfonate) (PSS), were grafted onto the convex surfaces of multiwalled carbon nanotubes (MWNTs) by surface-initiating ATRP (atom transfer radical polymerization) from the initiating sites previously anchored onto the convex surfaces of MWNTs. The grafted polyelectrolyte can be efficiently quantified by the feed ratio of monomer to MWNT-based macroinitiator, and the maximum amount of grafted polymer is higher than 55 wt%. The polyelectrolyte-coated MWNTs resembled core-shell structures justified by the TEM images of the samples obtained, which provided direct evidence for the covalent modification of MWNT. FTIR, ^{1}H NMR and TGA were used to determine the chemical structure of the resulting products. Comparison of UV–Vis spectra demonstrated that the products were water-soluble, and that PSS was more effective for improving the water solubility of carbon nanotubes. Using the polyelectrolyte- and carboxylic acid-functionalized MWNTs as templates, and poly(2-(*N*,*N*-dimethylaminoethyl) methacrylate (PDMAEMA)/hyperbranched polysulfone amine (HPSA) and PSS as polycation and polyanion, respectively, layer-by-layer (LbL) electrostatic self-assembly was conducted in order to explore the application of the functionalized nanotubes. It was found that the functionalized MWNTs have a high efficiency for loading polyelectrolytes by the LbL approach (the adsorbed polymer quantity is higher than 10 wt% in one assembling step). TEM observations showed that the assembled polymer shell on the MWNT surfaces was very even and flat.

Keywords: Carbon nanotubes; Multiwalled carbon nanotubes; Grafting from

1. Introduction

Various compounds and strategies have been used to functionalize carbon nanotubes (CNTs) in order to improve the solubility and processing of this promising tubular nanomaterials [1–5]. Easily soluble macromolecules, anchored to carbon nanotubes, have been shown to be more effective to improve the solubility, just like the 'life jacket' worn by carbon nanotubes.

To bond macromolecules to the surface, the 'grafting to' approach was firstly employed, by the esterification or amidation of the carboxylic groups on the surface of acid-treated CNTs, and thereby various polymers were successfully attached to the CNTs surfaces [1–6]. Recently, the 'grafting from' approach was newly developed to realize more effective functionalization of CNTs, which opens a possible route to well-controlled functionalization of CNTs, making the high density and even grafting easily accessible [7,8]. Significantly, atom transfer radical polymerization (ATRP) [9–11], a very powerful technique in functional macromolecular design and new material preparation, was successfully applied to the controlled functionalization of CNTs. Depending on ATRP, some homopolymers and copolymers such as poly(methyl methacrylate) (PMMA), poly(*n*-butyl acrylate) (P*n*BA), polystyrene (PS), and poly(methyl methacrylate)-*block*-poly(hydroxyethyl methacrylate) (PMMA-*b*-PHEMA) were grown on the surface of CNTs, including singlewalled carbon nanotubes (SWNTs)

* Corresponding author. Address: College of Chemistry and Chemical Engineering, Shanghai Jiao Tong University, 800 Dongchuan Road, Shanghai 200240, P. R. China. Tel.: +86 21 5474 2665; fax: +86 21 5474 1297.
E-mail address: chaogao@sjtu.edu.cn (C. Gao).

0032-3861/$ - see front matter © 2005 Elsevier Ltd. All rights reserved.
doi:10.1016/j.polymer.2005.01.037

and multiwalled carbon nanotubes (MWNTs) [8]. Thus, such in situ surface initiating ATRP provides us with a remarkable route to tailor the structure and properties of the modified CNTs and to construct novel CNT-based hybrid nanomaterials [8a].

Among polymers selected to bond with CNTs, water-soluble polymers are very attractive because the functions of both polymer and CNTs can be tailored to create one object and the as-prepared water-soluble nanocomposites have potential and versatile bioapplications [12]. Thus, cationic polyamines such as poly(propionylethylenimine-*co*-ethylenimine (PPEI-EI) [13], oligomeric and polymeric species containing poly(ethylene glycol) (PEG) blocks [14], poly (vinyl alcohol) (PVA) [15] and its copolymer poly(vinyl acetate-*co*-vinyl alcohol) (PVA-VA) [13a], and poly(*m*-aminobenzene sulfonic acid) (PABS) [16] were employed to functionalize CNTs, resulting in water-soluble CNT-polymer adducts. However, these macromolecules are attached to the surfaces of CNTs by the 'grafting to' approach, which is limited as regards grafting density, polymer quantity, and synthesis control-ability.

In this paper, two kinds of water-soluble anionic polyelectrolyte: polyacrylic acid (PAA) and poly(sodium 4-styrenesulfonate) (PSS), were grafted onto the surfaces of MWNTs by the 'grafting from' approach. The process was conducted by the surface-initiating ATRP from the initiating sites previously anchored to MWNTs. The grafting polymer amount can be efficiently controlled by the feed ratio of monomer to MWNT-supported macroinitiator (MWNT-Br). Ford and co-workers [17] have tried to functionalize SWNTs with PSS by free radical polymerization initiated with potassium persulfate. However, the loaded polymer quantity cannot be well controlled with such method.

It is recognized that polyelectrolyte is the term used to classify macromolecules that have many charged or chargeable groups when dissolved in a polar solvent: predominantly water. Polyelectrolytes such as poly (methacrylic acid) (PMAA), PAA, PSS and their block copolymers, have been widely used in the construction of organic–inorganic hybrid materials, nanostructured materials, and self-assembly [18]. Because of potential applications in separation technology, controlled drug delivery and release, and smart catalyst separation technology, polyelectrolytes have become one of the key knots in connecting material science, pharmacy, biochemistry and polymer science [18]. Hence, we believe that the controllable functionalization of MWNTs with water-soluble anionic polyelectrolytes will widely expand the applied fields of CNTs.

Furthermore, as an example of applied research for the polyeletrolyte-functionalized MWNTs, this paper has systematically investigated the layer-by-layer (LbL) self-assembly behavior with the functionalized MWNTs as the nano-substrate using linear poly(2-(*N*,*N*-dimethylaminoethyl) methacrylate (PDMAEMA) or hyperbranched poly (sulfone-amine) (HPSA) as polycations and PSS as polyanions, respectively. It was demonstrated that the MWNT surfaces have an extremely high efficiency for loading polyeletrolytes by this LbL self-assembly strategy, which will pave the way for CNTs to apply in the gene-delivery or other micro/nano transferring systems.

2. Experimental

2.1. Materials

Chemical vapor deposited (CVD) MWNTs were purchased from Tsinghua-Nafine Nano-Powder Commercialization Engineering Centre in Beijing. Carboxylic acid-functionalized MWNTs (MWNT-COOH) was prepared by oxidation of crude MWNTs with concentrated aqueous HNO_3 according to the previous procedure [8a]. TGA measurements indicated that the MWNT-COOH sample contained ca. 8 wt% of carboxylic acid groups. *tert*-Butyl acrylate (*t*BA) was purchased from Aldrich, the inhibitor having been removed by passage through an alumina column and distillation in vacuo. CF_3COOH, sodium 4-styrenesulfonate (NaSS) and ethyl 2-bromoisobutyrate were purchased from Aldrich and used as received. Cu(I)Br was obtained from Aldrich and purified by washing with glacial ethanoic acid, followed by ethanol and diethyl ether. *N*,*N*,*N*′,*N*′,*N*″- pentmethyldiethylenetriamine (PMDETA) was purchased from Acros and used as received. The 0.22 μ polycarbonate membrane filter was purchased from the Shanghai Reagents Company. *N*,*N*-dimethyl formamide (DMF) and other organic reagents or solvents were obtained from the Shanghai Reagents Company. The MWNT supported macroinitiator (MWNT-Br), containing 0.421 mmol initiator groups per gram MWNT-Br, was prepared following the published method [8a].

poly(2-(*N*,*N*-dimethylaminoethyl) methacrylate (PDMAEMA), with a number-average molecular weight (M_n) of 18,500 and a polydispersity index (PDI) of 1.5, was synthesized according to the published procedure with ethyl 2-bromoisobutyrate as initiator [11]. Hyperbranched poly (sulfone amine) (HPSA) with a M_n of 23,500 (PDI = 1.38) and a degree of branching (DB) of 57%, was synthesized by reaction of divinyl sulfone with 2-(1-aminoethyl)piperazine [19].

2.2. Instrumentation

FTIR spectra were recorded on a PE Paragon 1000 spectrometer. ^{1}H NMR spectra were recorded on a Varian Mercury Plus 400 MHz spectrometer. Transmission electron microscopy (TEM) analysis was performed on a JEOL JEL2010 electron microscope at 200 kV, and Hitachi H-7100 at 100 kV. The photograph of the samples placed in a solvent was recorded on a digital camera (Sony, DSC-S70). Thermal gravimetric analysis (TGA) was conducted on a PE

Table 1
The polymerization conditions and some results for grafting polymers from MWNT surfaces

Code	MWNT-Br mg/mmol	[I]/[Cu(I)]/[L]/[M]	Solvent	Temp. (°C)	Time/h	f_{wt}%[a]	Conv. (%)[b]	M_n	PDI
MWNT-P*t*BA1	50.3/0.0212	1:2:2:40	DMF	60	48	52	63	3,200[c]	
MWNT-P*t*BA2	50.8/0.0214	1:2:2:100	DMF	60	48	75	60	7,600[d]	
MWNT-PAA1			$CHCl_3$	RT	24	30			
MWNT-PAA2			$CHCl_3$	RT	24	35			
Pure PSS		1:1:1:100	DMF	130	30		88	18,500	1.50
MWNT-PSS1	51.2/0.0216	1:2:2:20	DMF	130	30	25	27		
MWNT-PSS2	50.1/0.0211	1:2:2:50	DMF	130	30	39	30		
MWNT-PSS3	49.6/0.0209	1:2:2:100	DMF	130	30	68	36		

[a] The polymer quantity of the product calculated from TGA data.
[b] The conversion of monomers, calculated from the yield of the corresponding product. For the samples of MWNT-polymer, conv.% = wt. of (polymer grafted MWNT-MWNT-Br)/wt. of monomer.
[c] Calculated from the integration ratio of terminal C*H*Br- to residual C*H*- of corresponding ^{1}H NMR spectra.
[d] Calculated from the integration ratio of terminal C*H*Br- to residual C*H*- of corresponding ^{1}H NMR spectra.

TGA-7 instrument with a heating rate of 20 °C/min in the nitrogen flow (10 mL/min). The molecular weight was measured on PE Series 200 gel permeation chromatography (GPC) with PSS as standards using HPLC-grade H_2O as eluent at a flow rate of 1 mL/min.

2.3. Synthesis of MWNT-PtBA

Typically, 50.3 mg of MWNT-Br (0.021 mmol Br), 6.0 mg (0.042 mmol) of CuBr, 7.3 mg (0.042 mmol) of PMDETA and 0.25 mL of DMF were placed in a 10 mL flask. After evacuating and thrice filling with Ar, 100.6 mg (0.78 mmol) of *t*BA were injected into the flask using a syringe. The flask was immersed in an oil bath at 60 °C. The mixture was stirred for 48 h, then diluted with $CHCl_3$ and vacuum-filtered using a 0.22 μ polycarbonate membrane. The filtered mass was dispersed in $CHCl_3$, then filtered and washed with $CHCl_3$. After drying overnight under vacuum, MWNT- P*t*BA1 (see Table 1) was obtained.

2.4. Synthesis of MWNT-PAA by hydrolysis of MWNT-PtBA

MWNT-PAA products were obtained by hydrolysing the P*t*BA blocks into PAA in the presence of CF_3COOH at room temperature [20,21]. Typically, 20.0 mg of as-prepared MWNT-P*t*BA and $CHCl_3$ (5 mL) were added to a 10 mL flask. Then CF_3COOH (0.5 mL) was added to the flask with a syringe. After 24 h, the product of MWNT-PAA was separated by evaporation of the solvent under vacuum, then dried in a vacuum overnight at 40 °C.

2.5. Preparation of pure PSS using ATRP

The ATRP polymerization of NaSS was carried out in DMF at 130 °C [11]. To a flask, 2.062 g (10 mmol) of SSNa, 14.3 mg (0.1 mmol) of CuBr, 17.3 mg (0.1 mmol) of PMDETA and DMF (4 mL) were added. The flask was sealed with a rubber bung, then evacuated and filled thrice with Ar. 19.5 mg (0.1 mmol) of ethyl 2-bromoisobutyrate dissolved in 0.1 mL of DMF was injected into the flask using a syringe. The flask was immersed in an oil bath at 130 °C, and the solution became dark brown. After 30 h, the solution was cooled and exposed to air. It was then diluted with 20 mL water and passed through an alumina column. The polymer was obtained by precipitation in acetone.

2.6. Preparation of MWNT-PSS

Typically, MWNT-PSS1 (Table 1), 51.2 mg of MWNT-Br, 7.0 mg (0.05 mmol) of CuBr, 8.6 mg (0.05 mmol) of PMDETA and DMF (0.5 mL) were placed in a 10 mL dry flask, which was then sealed with a rubber bung. The flask was evacuated and filled thrice with Ar. NaSS (50.0 mg, 0.24 mmol) dissolved in 0.5 mL of DMF was injected into the flask using a syringe. The flask was immersed in an oil bath at 130 °C, and the contents stirred for 30 h. The mixture was subsequently diluted with water and thrice vacuum-filtered using a 0.22 μ polycarbonate membrane. To ensure that no un-grafted polymer was mixed with the product, the filtered mass was dispersed in, then filtered and washed with water. The PSS-coated MWNT sample was obtained by filtration and drying overnight under vacuum.

2.7. LbL self-assembly on functionalized CNTs

We used as-prepared MWNT-COOH, MWNT-PAA and MWNT-PSS as the substrate, and PDMAEMA or HPSA and PSS as polycations and polyanioins, respectively, to investigate the LbL self-assembly behavior on the nano-surfaces. Taking sample LbL1 in Table 3 as a typical example to describe its preparation process, PDMAEMA (0.15 g), NaCl (5.8 g) and 100 mL of deionized water were placed in a 250 mL flask and stirred until PDMAEMA were completely dissolved. The pH value of the solution was adjusted to 3.7 by adding 2 M HCl. MWNT-COOH (80 mg) was then added to the as-prepared solution of PDMAEMA. The mixture was placed in an ultrasonic bath (40 kHz) for 3 min and stirred gently for 30 min. Then the solid was

separated by filtration through a 0.22 μ Millipore polycarbonate membrane filter and washed with deionized water three times. The resulting solid was added to 100 mL of an aqueous solution of PSS (1.5 g/L) and NaCl (1 M), followed with the same steps: ultrasonic dispersion, gently stirring, filtration and washing as described above. The subsequent sample was added to the HCl-treated aqueous solution of PDMAEMA (1.5 g/L) and NaCl (1 M) (pH = 3.7) and repeated the above steps. The ultimate sample (LbL1) was obtained by drying overnight in a vacuum at 50 °C.

3. Results and discussion

3.1. Preparation of MWNT-PtBA and MWNT-PAA

Scheme 1 shows the synthesis of MWNT-PAA from MWNT-supported macroinitiators (MWNT-Br). The experimental conditions and some results relating to the preparation of MWNT-P*t*BAs and MWNT-PAAs are summarized in Table 1.

The chemical structure of the polymer moieties on the MWNTs was determined by ^{1}H NMR and FTIR. In the ^{1}H NMR of MWNT-P*t*BA (Fig. 1), the unique proton signal of terminal units (C*H*Br) linked with the bromine atom can still be detected at ~4.15 ppm. The *tert*-butyl groups and tertiary-carbon protons of P*t*BA were identified as peaks at 1.43 and 2.21 ppm, respectively. Depending on the relative peak areas of the tertiary-carbon protons and proton signal of terminal units, the average degree of polymerization (DPs) for P*t*BA chains made with feed ratios (monomer/Br) of 40/1 and 100/1 were calculated to be 25 and 59, respectively, corresponding to the molecular weights of 3200 and 7600. Therefore, the chain length of P*t*BA building blocks coated on MWNTs can be efficiently controlled by the feed ratio. After hydrolysis of the P*t*BA blocks with CF_3COOH, the *tert*-butyl group peaks were hardly detectable in the corresponding ^{1}H NMR spectrum, which indicated the complete hydrolysis of *tert*-butyl groups and the realization of polyelectrolyte (PAA) grafted MWNTs.

The characteristic absorption bands (e.g., $\nu_{C=C}$, $\nu_{C=O}$, ν_{C-H}) for the resulting samples were found in their FTIR spectra (Fig. 2). For instance, the strong C=O stretch (ca. 1730 cm^{-1}), the characteristic carbonyl peak introduced by P*t*BA, obviously appeared in the spectrum of MWNT-P*t*BA, while only a weak absorption peak at ~1730 cm^{-1} was found in the spectrum of MWNT-Br. When the P*t*BA was hydrolized to PAA, a wide absorption band assigned to hydroxyl groups around 3440 cm^{-1} was significantly observed in the FTIR spectrum of MWNT-PAA. All these absorption data further suggested that the synthesis of MWNT-P*t*BA and the hydrolysis of P*t*BA had been successful.

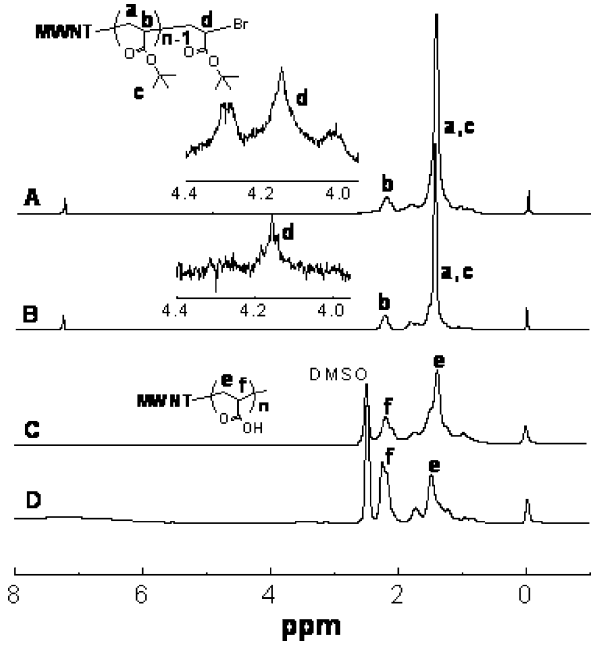

Fig. 1. ^{1}H NMR spectra of MWNT-P*t*BA1 in $CDCl_3$ (A), MWNT-P*t*BA2 in $CDCl_3$ (B), MWNT-PAA1 in DMSO-d_6 (C), and MWNT-PAA2 in DMSO-d_6 (D).

The TGA measurements provided further evidence regarding the content and species of grafted polymer on the surfaces of MWNTs, because the polymer and MWNTs parts have different thermal-stability [20,22]. In the TGA curve of MWNT-P*t*BA, the weight loss in the 160–290 °C range (onset ~232 °C) was attributed to decomposition of the *tert*-butyloxygen moieties of P*t*BA blocks, and the weight loss between 290 and 460 °C assigned to the degradation of residual P*t*BA segments. In the TGA curve of MWNT-PAA, a continuous weight loss tendency was detected which indicated that PAA segments had much lower thermal stability as compared with P*t*BA ones because of their carboxylic acid groups resulting from hydrolysis of *tert*-butyl groups [20].

One of the merits of this in situ ATRP approach is the even grafting on the surfaces of MWNTs [8a,22]. Here, the

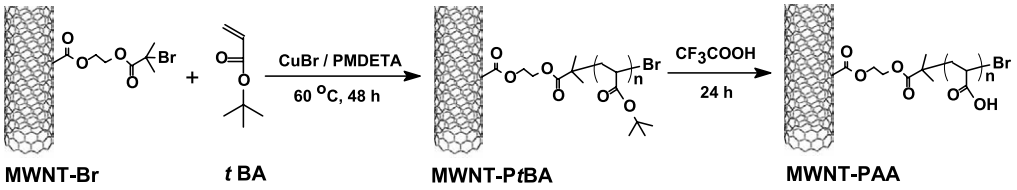

Scheme 1.

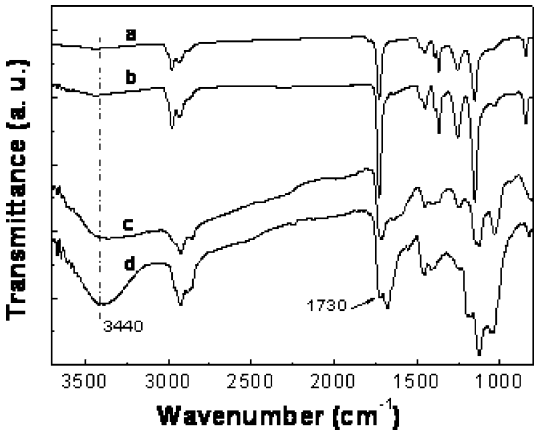

Fig. 2. FTIR spectra of MWNT-P*t*BA1 (a), MWNT-P*t*BA2 (b), MWNT-PAA1 (c), and MWNT-PAA2 (d).

morphological structure of MWNT-PAA was also recognized by TEM (see Fig. 3). It was also found that the tubes were coated evenly with polymer grafts, and that all of the tubes were wrapped drastically if compared with the crude MWNTs. Such ideal coating resulted from the covalent linkage of polymer layers in this in situ polymerisation strategy. If the polymer was only mixed with MWNTs, such complete wrapping was not observed in our experiments, and the individual phases of polymers and MWNTs were generally found during TEM observation.

3.2. Preparation of MWNT-PSS

Scheme 2 shows the synthesis for grafting PSS from the surfaces of MWNTs. The experimental conditions and some results of MWNT-PSS are summarized in Table 1. It was demonstrated that NaSS is an ATRP-active monomer [11]. In our comparable blank experiment, the pure PSS made from a typical ATRP condition without MWNT-Br had a M_n of 18,500 and a PDI of 1.50. The monomer conversion exceeded 85%. However, the monomer conversion in the preparation of MWNT-PSSs initiated from MWNT-Br was only ~25–40%, i.e. much lower than that of pure PSS.

Again, the grafted polymer amount of MWNT-PSSs can be calculated from corresponding TGA curves (Fig. 4). The weight loss below 500 °C for the pure PSS sample is 37.5%, which corresponds to the decomposition of the main chains and benzene rings. With the weight loss of pure PSS below 500 °C as the reference, the calculated polymer amounts, MWNT-PSSs, were ~25, 39, and 68 wt%, respectively. Therefore, the grafted PSS quantities can be also well controlled by this 'grafting from' strategy. It should be noted that some of the weight loss below 200 °C may be due to adsorbed water, and thus the calculations based on the TGA data had a probable error of 5–10%.

Fig. 5 illustrates the FTIR spectra of crude MWNTs and MWNT-PSSs. Compared with the MWNTs, the PSS grafted MWNTs showed quite different spectra. The aromatic C–H stretch was observed as peaks at 3098 and 1580–1602 cm^{-1},

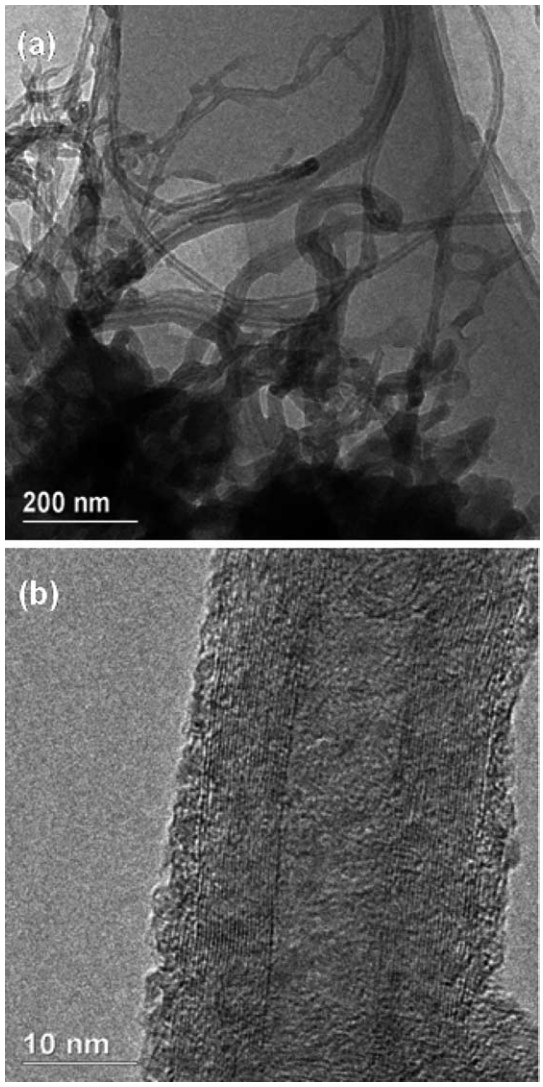

Fig. 3. TEM images of MWNT-PAA1 at low magnification (a) and high magnification (b).

and the aliphatic C–H stretch of the polymer backbones was observed at 2921 and 2848 cm^{-1}. The absorption peaks of the O=S=O stretch appeared at 1208 and 1156 cm^{-1}. The S–O and C–S stretches appeared at 663 and 641 cm^{-1}, respectively. Because MWNT-PSS can form a complex with water, or adsorb water, a strong O–H stretch was observed at 3436 cm^{-1} for MWNT-PSS samples.

To answer the question whether the PSS had been covalently grafted onto the convex surface of MWNT or not, TEM was one of the most directly powerful tools. Two typical TEM images of sample MWNT-PSS2 are shown in Fig. 6. In the lower magnification image (Fig. 6(a)), it can be seen that almost all of the tubes were evenly covered with a polymer shell. In the high-resolution image (Fig. 6(b)), the core-shell structure of a polymer-functionalized tube was clearly observed. The core with graphite sheets corresponded to the tubes and the shell layer attached tightly to the outer graphite sheet attributed to the polymer grafts. In

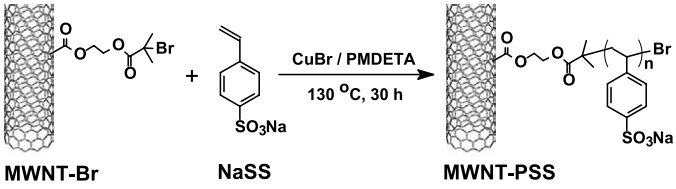

Scheme 2.

this image, the thickness of the grafted polymer layer is ~6 nm for the top side and ~3 nm for the bottom. Some of the polymer chains may be partially stretched out from the tube surface due to the high grafting density, resulting in such high thickness of polymer layer.

3.3. Solubility of the polyelectrolyte-functionalized MWNTs

The solubility or dispersibility of the functionalized MWNTs strongly depends on the structure and amounts of the grafted organic moieties [22a]. As implied by the structure of the bonded polymers, the MWNT-P*t*BA displayed relatively good solubility in weakly polar and nonpolar solvents such as THF, $CHCl_3$ and toluene, but poor solubility in strongly polar solvents such as DMF and water. In contrast, after hydrolysis of the P*t*BA blocks, the MWNT-PAA can be dissolved easily in water, but is not soluble in weakly polar and nonpolar solvents, as anticipated. Similarly to the MWNT-PAA, MWNT-PSS samples showed good solubility in water and poor solubility in organic solvents, especially the weakly polar and nonpolar solvents, because of the grafted polyelectrolytes.

To assess the water solubility of the resulting MWNT-based polyelectrolytes, aqueous solutions of the samples at a certain concentration were prepared. Black and stable solutions appeared (Fig. 7, inset), indicating that the polyelectrolytes grown from MWNTs had good solubility in water, and the covalent linkage of hydrophilic PAA or PSS chains to the MWNT altered the interfacial property of carbon nanotubes. The soluble brush-like polymer chains pull the relatively huge MWNT backbones into the water phase and help enhance the solubility of carbon tubes. But when a beam of light spread through the solution, the 'Tyndall effect' could be observed. The diameter of some nanocomposite particles must be larger than 200 nm, which demonstrated the existence of aggregation between functionalized nanotubes.

To obtain a semi-quantitative result for the water solubility of the products, a UV–Vis spectrophotometer was used to record the absorbance in water solution (see Fig. 7). The absorbance (A) of the polyelectrolyte-grafted MWNTs in water is much higher than that of acid-treated MWNT (MWNT-COOH), and the greater the bonded polymer amount, the higher the absorbance. The absorbance values at 600 nm (A_{600}) for the resulting samples are given in Table 2. It is found that the absorbance of MWNT-PSS is significantly higher than that of MWNT-PAA because of the higher solubility of PSS in water than that of PAA grafts.

Fig. 8 displays the absorption spectra of MWNT-PSS3 at different concentrations. The absorbance is in direct proportion to the sample concentration, in agreement with Beer's law.

3.4. LbL self-assembly on the functionalized MWNT surfaces

Because of their high water-solubility and high anion density, the resulting polyeletrolyte-functionalized MWNTs have potential applications in biomaterials and micro-/nono- devices and materials, etc. [12,18]. As an important application aspect, this work used the polyeletrolyte-functionalized MWNTs as templates for further surface

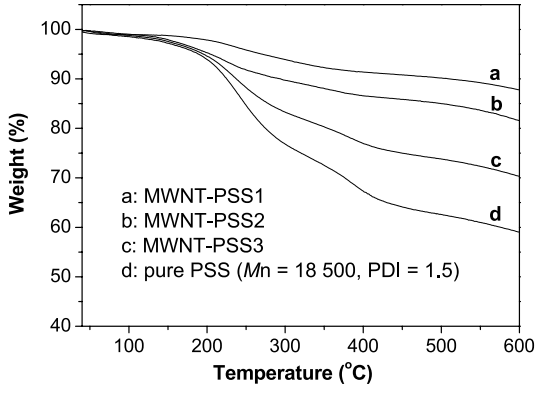

Fig. 4. TGA curves of PSSNa, MWNT-PSS1, MWNT-PSS2, and MWNT-PSS3.

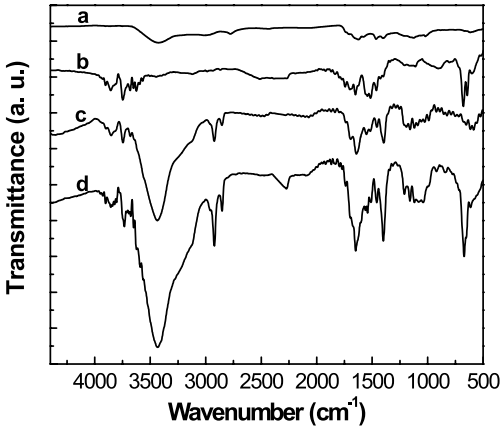

Fig. 5. FTIR spectra of MWNT (a), MWNT-PSS1 (b), MWNT-PSS2 (c), and MWNT-PSS3 (d).

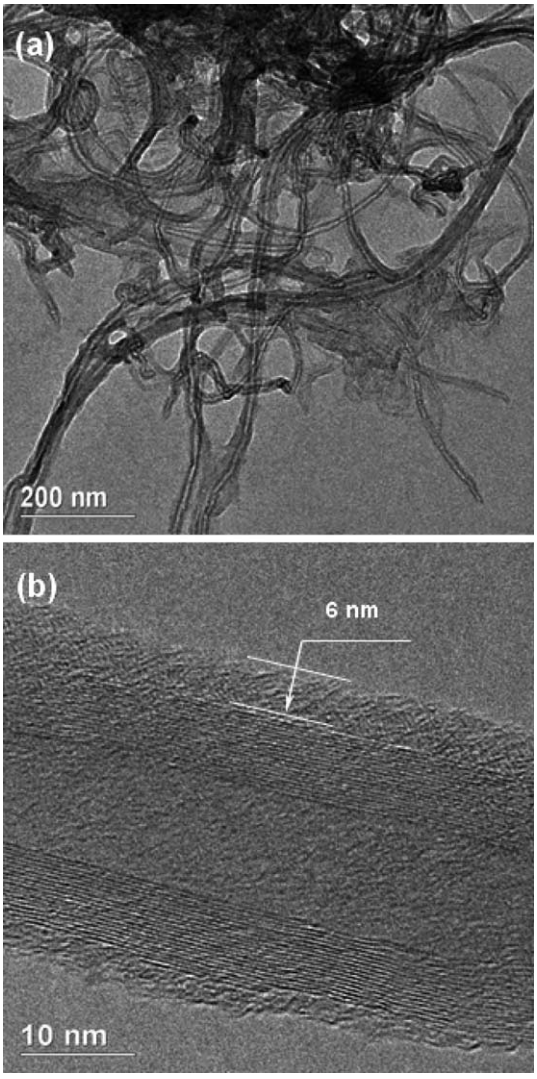

Fig. 6. TEM images of MWNT-PSS2 at low magnification (a) and high magnification (b).

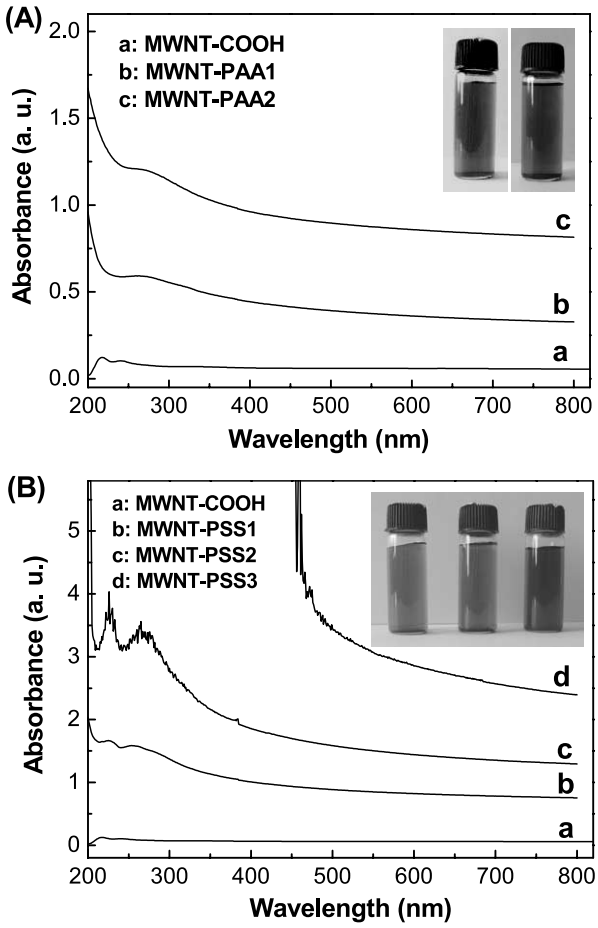

Fig. 7. (A) UV–Vis spectra of MWNT, MWNT-PAA1, and MWNT-PAA2 in water solution; (B) UV–Vis spectra of MWNT-PSS1, MWNT-PSS2, and MWNT-PSS3 in water solution. Insert of (A): the photographs of the sample CS MWNT-PAA1 (left) and MWNT-PAA2 (right) placed in water at a concentration of 1 mg sample per 5 mL water. Insert of (B): the photographs of the samples MWNT-PSS1 (left), MWNT-PSS2 (middle) and MWNT-PSS3 (right) placed in water at a concentration of 1 mg sample per 5 mL water.

functionalization by the LbL self-assembly approach on the basis of their surface charges.

The LbL approach, based on the electrostatic attraction between oppositely charged species, is a crucial method for fabricating new compounds and novel structures, for synthesizing hybrid materials, and for modifying solid surfaces [23]. One of its major advantages is allowing precise and uniform control over the thickness and properties of the assembled layers because the thickness of the multilayer structure generally increases linearly with the number of adsorbed layers. Two- and three-dimensional substrates such as silicon wafer, silica flat, gold colloid and other nanoparticles, have been widely employed as the supporters or templates in the LbL self-assembly [24]. Evidently, one-dimensional CNTs can play two different roles in the LbL processing: substrates to load polyelectrolytes on or polyanions to coat polycation-modified films. As regarding nanosubstrates, Smalley and coworkers [25] have reported that certain polyelectrolytes can adsorb directly on CNTs, but the formed hybrids were unstable as usual and leached with time. Therefore, Noy et al. [26] introduced charged species (amino groups) on CNT surfaces

Table 2
The absorbance at 600 nm (A_{600}) of the samples with a concentration of 1 mg sample per 5 mL water

Item	MWNT-COOH	MWNT-PAA1	MWNT-PAA2	MWNT-PSS1	MWNT-PSS2	MWNT-PSS3
A_{600}	0.055	0.36	0.82	0.86	1.42	2.85
R_{600}[a]	1.00	6.55	14.91	15.64	25.82	51.82

[a] The ratio of A_{600} of the sample to A_{600} of acid-treated MWNT (MWNT-COOH).

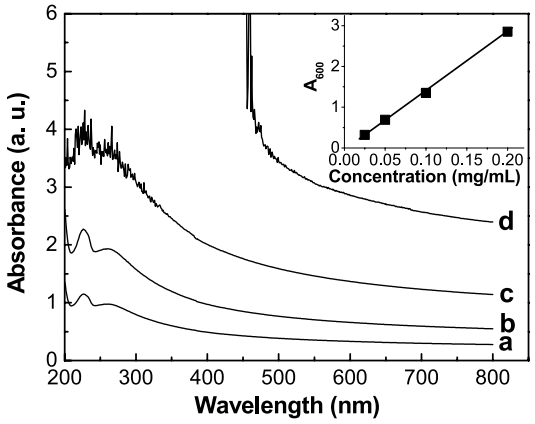

Fig. 8. UV–Vis absorption spectra of MWNT-PSS3 in water solution at concentrations of 0.025 (a), 0.05 (b), 0.10 (c), and 0.20 (d) mg/mL. Insert: the absorbance at 600 nm of MWNT-PSS3 as a function of concentration.

by the so-called π–π stacking between pyrene rings and CNTs using 1-pyrenepropylamine hydrochloride ($PyrNH_3$) as the 'bridges', following adsorption of polyanions and polycations, in order to obtain robust and stable nanohybrids. This improvement definitely set up a novel route to functionalize CNTs, and open a door to fabricate CNT-based nanodevices and nanomaterials by electrostatic self-assembly on CNT surfaces [26]. However, three limitations are concomitant with this route. Firstly, the non-covalently adsorbed pyrene derivative-anchors on CNT surfaces would de-adsorb sometimes, especially in the case of loading extra masses, which leads to de-functionalization and uneven coating [27]. Secondly, the adsorbed polymer shell is rough because of the low coverage of pyrenes on CNT surfaces, which significantly influences the uniformity of the assembled layers [26,28]. Finally, it is relatively difficult to achieve high quantity as well as highly even coating due to the aforementioned de-functionalization and rough coating. On the other hand, CNTs can also play the role of polyanions because the tubular surfaces can be oxidized to generate plenty of carboxylic acid groups. Taking advantage of the strong attractions between oxidized CNTs and cationic compounds, as well as the outstanding mechanical strength of CNTs, Mamedov et al. prepared CNT-based composites with good mechanical properties [29]. Therefore, high density and highly even assembled nanowires would be expected by the LbL approach using the covalently ionic CNTs, rather than noncovalently functionalized ones, as the templates. This topic will be systematically discussed by the following contents of this article. In addition, it is easy to understand that the linear polymer chains can adsorb smoothly along the tubular surface. A question appears immediately: what's the result for the CNT-supported electrostatic self-assembly if three-dimensional dendritic macromolecules [30] are used as the polyeletrolytes? This question will also be answered in the following discussions.

The LbL self-assembly procedure on MWNT surfaces is shown in Scheme 3. Three kinds of functionalized CNTs: MWNT-COOH, MWNT-PAA1 and MWNT-PSS1, were employed as the templates. Linear PDMAEMA and hyperbranched poly(sulfone amine) were selected as polycations to compare their electrostatic self-assembly efficiency.

Table 3
Depositing polyelectrolyte layers on MWNT surfaces via layer-by-layer electrostatic self-assembly approach

Sample	Substrate	Polycation		f_{wt}%[a]
		PDMAEMA (mg/mL)	HPSA (mg/mL)	
LbL1	MWNT-COOH	1.5		40
LbL2	MWNT-COOH		1.7	36
LbL3	MWNT-PAA1	1.5		75
LbL4	MWNT-PAA1		1.7	70
LbL5	MWNT-PSS1	1.5		78
LbL6	MWNT-PSS1		1.7	72

[a] The weight loss fraction of polymers calculated from TGA results.

The loaded polymer quantity was determined by TGA measurements. The results are summarized in Table 3. As a typical example, Fig. 9 displays the TGA weight loss curves of crude MWNTs, MWNT-COOH, and samples LbL1 and LbL2. The first weight-loss stage occurs below ~220 °C, which is assigned to the decomposition of carboxyl groups of MWNT-COOH. The second weight-loss stage between 220 °C and 460 °C is attributed to the decomposition of PDMAEMA (for LbL1), HPSA (for LbL2) and PSS. 40% and 36% weight losses were observed for LbL1 and LbL2, respectively, although only three alternating adsorption steps were carried out. This indicates that, (1) MWNTs have extremely high efficiency for loading polyeletrolytes by the LbL approach, and over 10 wt% of polyelectrolytes can be loaded on CNT surfaces in one adsorption step; (2) globular hyperbranched macromolecules can also be assembled on the nanotube surfaces with a high efficiency, but the loaded quantity is a little lower than that of linear polycations (ca. 2–3 wt% per step); and (3) entanglement between tube and polymer chains can facilitate the LbL self-assembly, but the electrostatic attraction between opposite charges plays the key role. These outcomes are further approved by other experiments (LbL3-LbL6) (see Table 3).

The chemical structure of samples was characterized by FTIR (Fig. 10). The characteristic peak C–H strecting appears at 2950 cm^{-1} in the spectra of LbL1 and LbL2, while no absorption band is found in this area in the spectrum of MWNT-COOH (Fig. 10(A)). The C=O stretching absorption band of PDMAEMA is observed in the spectrum of LbL1. Compared with the spectrum of MWNT-COOH, the bands at ca. 1100 cm^{-1} of LbL1 and LbL2 are much stronger, which results from the contribution of C–O (PDMAEMA) and O=S=O (HPSA) absorption of polyelectrolytes. In the spectra of LbL3-LbL6, obvious absorption bands at ca. 1100 cm^{-1} are also observed, which corresponds to C–O (PDMAEMA) or

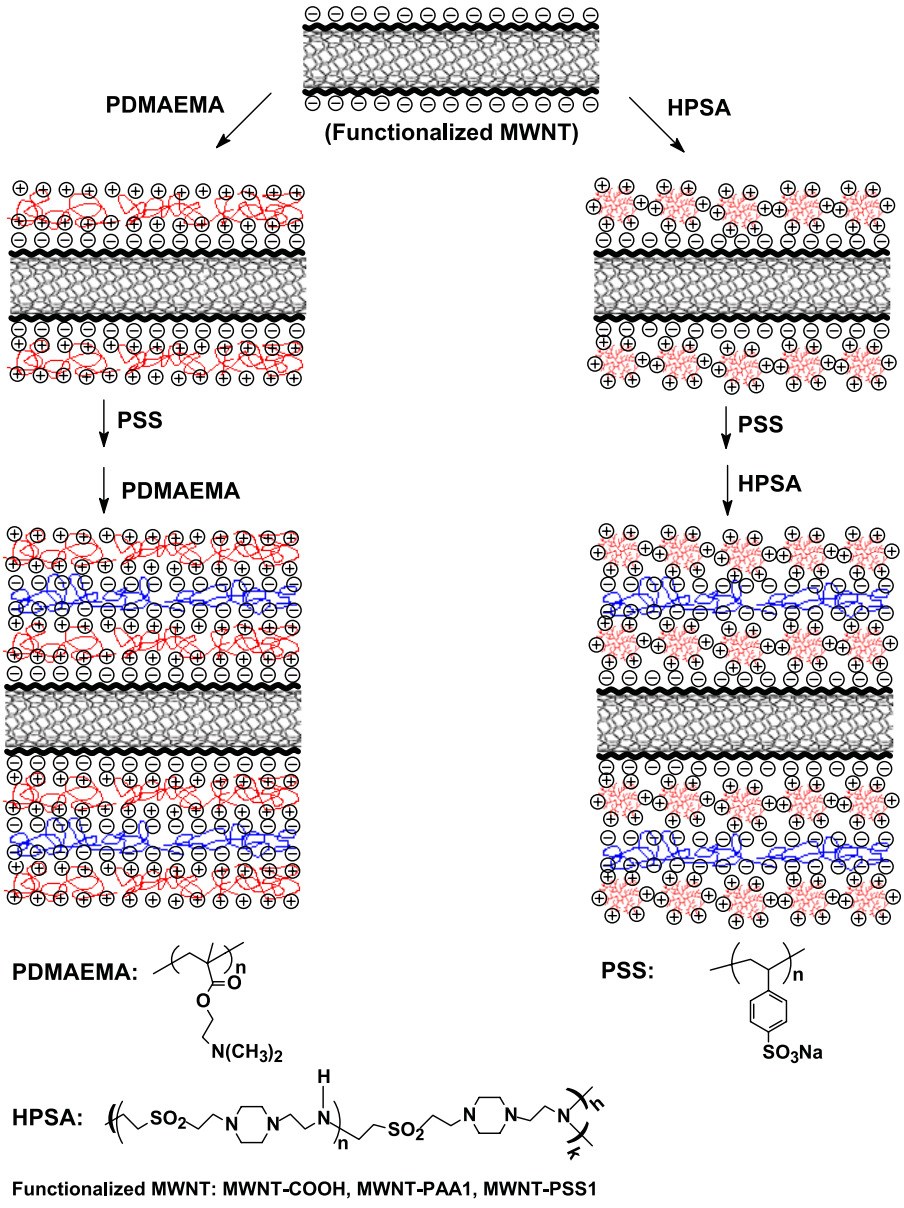

Scheme 3.

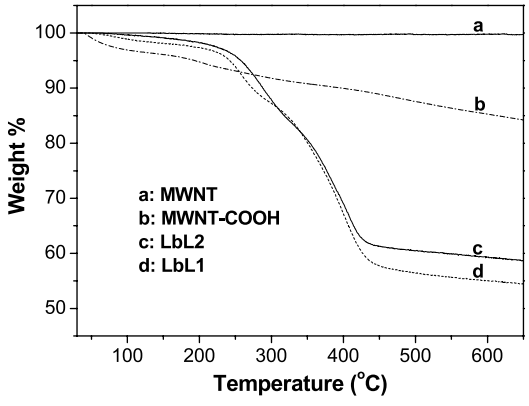

Fig. 9. TGA curves of crude MWNTs (a), MWNT-COOH (b), LbL2 (c) and LbL21 (d).

O=S=O (HPSA) stretching vibration of the loaded polyelectrolytes (Fig. 10(B) and (C)).

The effect of the LbL self-assembly to functionalize CNTs can be evaluated by TEM and SEM measurements. Fig. 11 shows the representative TEM images of sample LbL1 (images a–e) and crude MWNTs (images f and g). It is found that the assembled polymer shell is quite thorough and even whenever in view of a large area (low magnification, images a–c) or local points (higher magnification, images d and e). After MWNT was fully wrapped with polymers, a core-shell structure would be formed with MWNT and polymer as cylindrical core and hairy shell, respectively, according to our former observations. This core-shell structure can be viewed under TEM at high magnification because of different density and atom

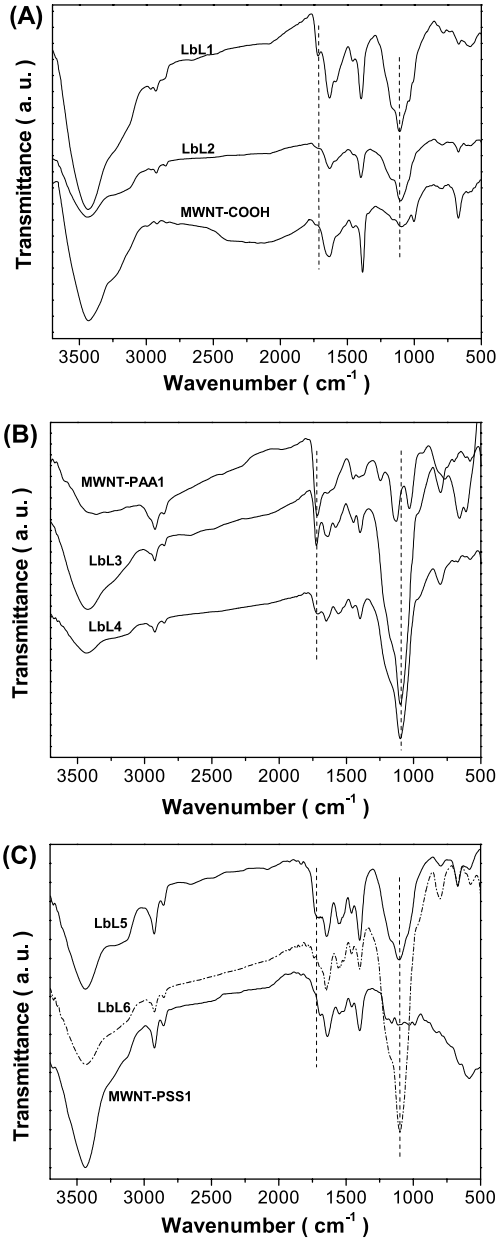

Fig. 10. (A) FTIR spectra of LbL1, LbL2 and MWNT-COOH. (B) FTIR spectra of MWNT-PAA1, LbL3 and LbL4. (C) FTIR spectra of LbL5, LbL6 and MWNT-PSS1.

arrangement between tubes and polymers. For the samples made by the LbL approach, such core-shell structure was also observed clearly by TEM (images d and e). Under HRTEM at a high magnification, the tubular structure of the MWNT core can be detected, and the individual phases of tubes and polymers can also be evidently distinguished from the different gray (image e). Significantly, the outer side of the polymer layer is quite smooth and flat, and the thickness of the polymer shell is relatively uniform, which further indicates that the distribution of carboxylic acid groups on MWNT surfaces is relatively symmetrical and the LbL self-assembly effect on the nanowires is very good. By comparison, the images of crude MWNTs are also given in Fig. 11 (images f and g), showing a clear surface and no hairy shell structure.

Fig. 12 displays the representative TEM images of other LbL self-assembly samples. Interestingly, the hyperbranched polymers were also assembled on the tube surfaces very evenly despite their three-dimensional globular architecture (images a–c). Compared with the covalent coating of hyperbranched polymers on MWNT surfaces, this LbL assembling exhibits even a slightly better performance in terms of uniformity because of the strong attraction between opposite charges. Again, the core-shell structure was distinctly observed at higher magnifications (images b and c). For the samples templated from polyeletrolytes-grafted MWNTs (LbL3-LbL6), the assembled polymer quantity is so high that the polymer becomes a continuous phase (images d1, e, f, h). Estimating from the isolated or extended parts (images d2, e and g), we can find that, (1) the assembled polymer shell is also quite even and flat, (2) the thickness of the polymer shell is very high (>10 nm), and (3) the further coating effect for previous polymer-functionalized MWNTs via this LbL approach is also very good whenever the assembled polymers are one-dimensional linear or three-dimensional dendritic. Similar to the case of covalent grafting, some of the polymer chains adsorbed on the tube surface may be partially stretched out from the nanosurface due to the high adsorbing density or quantity, resulting in such high thickness of polymer layer. Clearly, detailed studies need to be conducted to fully understand how the polymer chains arrange on the cylindrical nanosurface.

The morphology and assembling effect were further evaluated by SEM measurements. Fig. 13 shows the SEM images of crude MWNTs (images a and b) and samples of LbL1 (images c and d) and LbL2 (images of e and f). For the crude MWNTs, the individual tubes can be clearly viewed. After assembling of polymers on the tube surfaces, the resulting solid became a composite in which the tubes are evenly dispersed. This suggests that CNT/polymer composites can be easily obtained by the LbL electrostatic self-assembly approach. Because the dendritic polymers can play the role of molecular vessels to load guest compounds such as organic dyes and inorganic ions [31], this composite has huge potential in the nano-, bio- and supramolecular chemistry fields. The relevant work is in progress, and will be reported later.

4. Conclusions

Two kinds of water-soluble anionic polyelectrolytes were successfully grafted onto the surface of MWNTs by in situ ATRP ‘grafting from’ process, resulting in the formation of core-shell nanostructures, with the PAA or PSS as the brush-like or hairy shell, and the MWNT as the hard backbone. The covalent bonding of polyelectrolytes to the MWNT dramatically improved the water solubility of

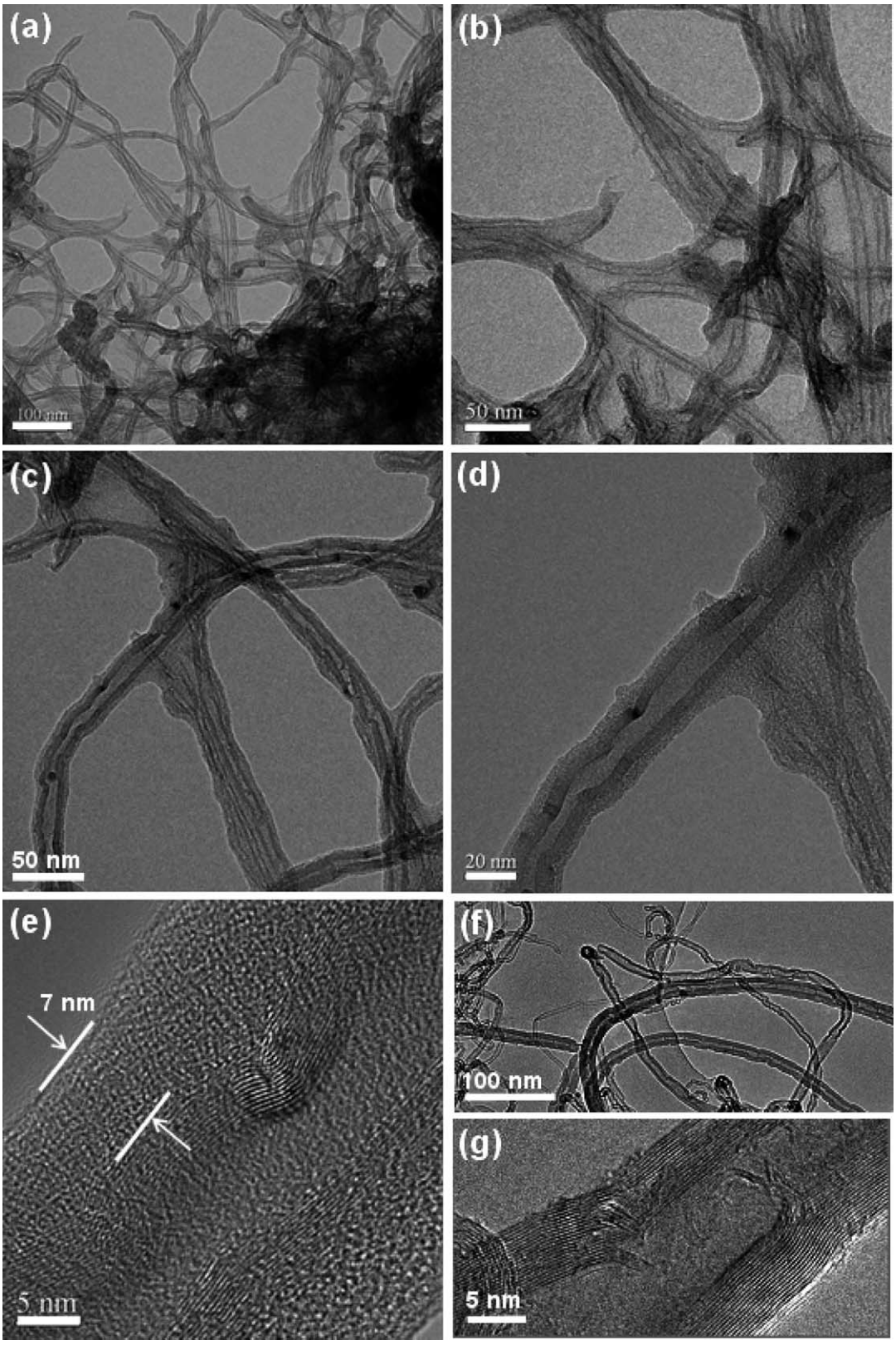

Fig. 11. Representative TEM images (200 kV) of sample LbL1 ((a)–(e)) and crude MWNTs ((f) and (g)) at different magnification.

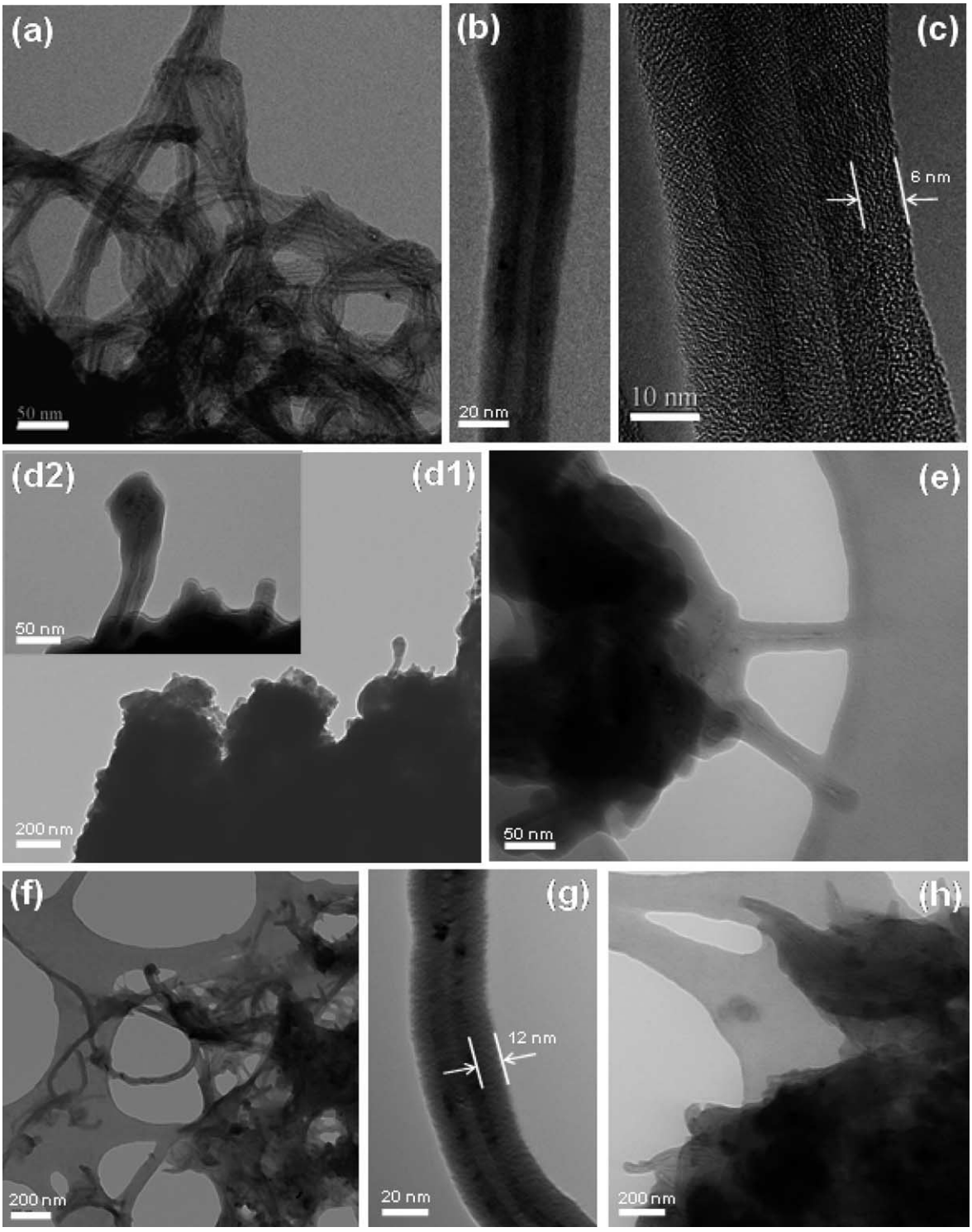

Fig. 12. Representative TEM images of LbL2 (a–c, 200 kV), LbL3 (d1 and d2, 100 kV), LbL4 (e, 100 kV), LbL5 ((f) and (g), 100 kV), and LbL6 ((h) 100 kV).

MWNTs, which may shed light on the further exploring and application of carbon nanotubes in the field of self-assembly, drug delivery and release, smart nanomaterials, and so forth.

Based on the MWNT-supported hybrid one-dimensional (1D) nano-polyelectrolytes and carboxylic acid-functionalized MWNTs, self-assembly nanowires were easily fabricated by the well-known layer-by-layer approach. The loading efficiency on the nanosurface is very high, which is a higher 10 wt% of polymer quantity in one deposition step. The assembled polymer shell on functionalized MWNT surfaces was quite even and flat.

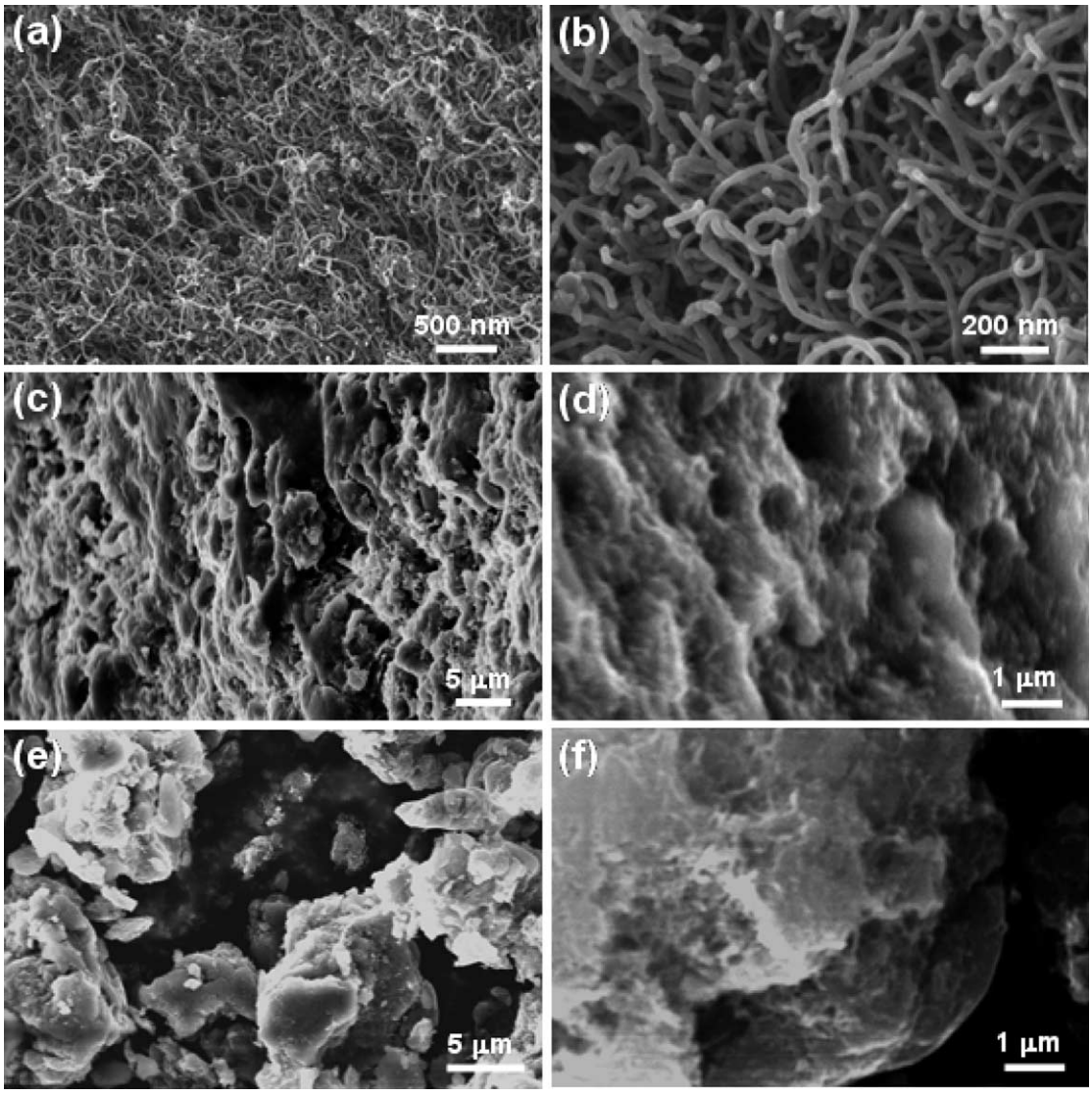

Fig. 13. Representative SEM images of crude MWNTs ((a) and (b)), LbL1 ((c) and (d)), and LbL2 ((e) and (f)).

The realization of CNTs/polyelectrolytes nanocomposites via the simple LbL approach will pave the way for the carbon nanotubes in the applications of nanomaterials and supramolecular chemistry.

Acknowledgements

We acknowledge financial support from the National Natural Science Foundation of China (Nos 50473010 and 20304007), Fok Ying Tung Education Foundation (No. 91013), Rising-Star Program Foundation of Shanghai (No. 03QB14028), and EPSRC (RKT4). We thank Dr David Walton and Prof Sir Harry Kroto in the University of Sussex for helpful discussions, and Mr J. Thorpe and Mr D. Randall (Sussex) for assistance with TEM and SEM facilities.

References

[1] (a) Dai L, Mau AWH. Adv Mater 2001;13:899.
(b) Banerjee S, Kahn MGC, Wong SS. Chem Eur J 2003;9:1898.
(c) Sun Y-P, Fu K, Lin Y, Huang W. Acc Chem Res 2002;35:1096.
(d) Niyogi S, Hamon MA, Hu H, Zhao B, Bhowmik P, Sen R, et al. Acc Chem Res 2002;35:1105.
[2] (a) Kang Y, Taton TA. J Am Chem Soc 2003;125:5650.
(b) Carrillo A, Swartz JA, Gamba JM, Kane RS. Nano Lett 2003;3:1437.
(c) Feng L, Li H, Li F, Shi Z, Gu Z. Carbon 2003;41:2385.
(d) Asai M, Fujita N, Sano M, Shinkai S. J Mater Chem 2003;13:2145.
[3] (a) Freitag R, Garret-Flaudy F. Langmuir 2002;18:3434.
(b) Xiao D, Wirth MJ. Macromolecules 2002;35:2919.
[4] (a) Jones DM, Smith JR, Huck WTS, Alexander C. Adv Mater 2002;14:1130.
(b) Kim DJ, Heo J, Kim KS, Choi IS. Macromol Rapid Commun 2003;24:517.
(c) Zhu M, Wang L, Exarhos GJ, Li ADQ. J Am Chem Soc 2004;126:2656.

[5] (a) Oupicky D, Reschel T, Konak C, Oupicka L. Macromolecules 2003;36:6863.
(b) Garnweitner G, Smarsly B, Assink R, Ruland W, Bond E, Brinker CJ. J Am Chem Soc 2003;125:5626.
[6] (a) Sun Y-P, Liu B, Moton DK. Chem Commun 1996;2699.
(b) Sano M, Kamino A, Shinkai S. Angew Chem Int Ed 2001;40: 4661.
[7] (a) Viswanathan G, Chakrapan N, Yang H, Wei B, Chung H, Cho K, et al. J Am Chem Soc 2003;125:9258.
(b) Wu W, Zhang S, Li Y, Li J, Liu L, Qin Y, et al. Macromolecules 2003;36:6286.
(c) Shaffer MSP, Koziol K. Chem Commun 2002;2074.
[8] (a) Kong H, Gao C, Yan D. J Am Chem Soc 2004;126:412.
(b) Yao Z, Braidy N, Botton GA, Adronov A. J Am Chem Soc 2003; 125:16015.
(c) Qin S, Qin D, Ford WT, Resasco DE, Herrera JE. J Am Chem Soc 2004;126:170.
(d) Baskaran D, Mays JW, Bratcher MS. Angew Chem Int Ed 2004; 43:2138.
[9] (a) Wang J, Matyjaszewski K. J Am Chem Soc 1995;117:5614.
(b) Coessens V, Pintauer T, Matyjaszewski K. Prog Polym Sci 2001; 26:337.
(c) Qiu J, Charleux B, Matyjaszewski K. Prog Polym Sci 2001;26:2083.
(d) Matyjaszewski K, Xia J. Chem Rev 2001;101:2921.
[10] (a) Liu T, Jia S, Kowalewski T, Matyjaszewski K, Casado-Portilla R, Belmont J. Langmuir 2003;19:6342.
(b) Mandal TK, Fleming MS, Wait DR. Nano Lett 2002;2:3.
(c) Wang Y, Teng X, Wang J, Yang H. Nano Lett 2003;3:789.
(d) Carrot G, Diamanti S, Manuszak M, Charleux B, Vairon J-P. J Polym Sci, Part A: Polym Chem 2001;39:4294.
[11] (a) Choi C, Kim Y. Polym Bull 2003;49:433.
(b) Liu P, Liang D, Tong Z, Liu X. Macromolecules 2002;35:1487.
[12] Lin Y, Taylor S, Li H, Fernando S, Qu L, Wang W, Gu L, Zhou B, Sun Y-P. J Mater Chem 2004;14:527.
[13] (a) Riggs JE, Guo Z, Carroll DL, Sun Y-P. J Am Chem Soc 2000;122: 5879.
(b) Riggs JE, Walker DB, Carroll DL, Sun Y-P. J Phys Chem B 2000; 104:7071.
[14] For example, see: (a) Huang W, Fernando S, Allard LF, Sun Y-P. Nano Lett 2003;3:565.
(b) Sano M, Kamino A, Okamura J, Shinkai S. Langmuir 2001;17:5125.
(c) Kahn MGC, Banerjee S, Wong SS. Nano Lett 2002;2:1215.
[15] Lin Y, Zhou B, Fernando KAS, Allard LF, Sun Y-P. Macromolecules 2003;36:7199.
[16] Zhao B, Hu H, Haddon HC. Adv Funct Mater 2004;14:71.
[17] Qin S, Qin D, Ford WT, Herrera JE, Resasco DE, Bachilo SM, Weisman RB. Macromolecules 2004;37:3965.
[18] For example, see: (a) Mori H, Müller AHE. Prog Polym Sci 2003;28: 1403.
(b) Bertrand P, Jonas A, Laschewsky A, Legras R. Macromol Rapid Commun 2000;21:319.
(c) Decher G, Eckle M, Schmitt J, Struth B. Curr Opin Colloid Interface Sci 1998;3:32.
(d) Lvov Y, Ariga K, Ichinose I, Kunitate T. J Am Chem Soc 1995; 117:6117.
[19] (a) Yan D, Gao C. Macromolecules 2000;33:7693.
(b) Gao C, Yan D. Macromolecules 2001;34:156.
[20] Kong H, Gao C, Yan D. J Mater Chem 2004;14:1401.
[21] Cheng GL, Boker AA, Zhang MF, Krausch G, Müller AHE. Macromolecules 2001;34:6883.
[22] (a) Kong H, Gao C, Yan D. Macromolecules 2004;37:4022.
(b) Kong H, Li W, Gao C, Yan D, Jin YZ, Walton DRM, Kroto HW. Macromolecules 2004;37:6683.
[23] Decher G. Science 1997;277:1232.
[24] For example, see: (a) Gittins DI, Caruso F. J Phys Chem B 2001;105: 6846.
(b) Mayya KS, Schoeler B, Caruso F. Adv Funct Mater 2003;13:183.
(c) Hong X, Li J, Wang M, Xu J, Guo W, Li J, et al. Chem Mater 2004;16:4022.
(d) Hammond PT. Adv Mater 2004;16:1271.
(e) von Klitzing R, Tieke B. Adv Polym Sci 2004;165:177.
(f) Caruso F. Top Curr Chem 2003;227:145.
[25] O'Connell MJ, Boul P, Ericson LM, Huffman C, Wang YH, Haroz E, et al. Chem Phys Lett 2001;342:265.
[26] Artyukhin AB, Bakajin O, Stroeve P, Noy A. Langmuir 2004;20: 1442.
[27] Gomez FJ, Chen RJ, Wang DW, Waymouth RM, Dai HJ. Chem Commun 2003;190.
[28] Liu L, Wang TX, Li JX, Guo ZX, Dai LM, Zhang DQ, et al. Chem Phys Lett 2003;367:747.
[29] (a) Mamedov AA, Kotov NA, Prato M, Guldi DM, Wicksted JP, Hirsch A. Nat Mater 2002;1:190.
(b) Rouse JH, Lillehei PT. Nano Lett 2003;3:59.
(c) Kim B, Park H, Sigmund WM. Langmuir 2003;19:2525.
[30] (a) Gao C, Yan D. Prog Polym Sci 2004;29:183.
(b) Mori H, Müller AHE. Top Curr Chem 2003;228:1.
(c) Jikei M, Kakimoto M. Prog Polym Sci 2001;26:1233.
(d) Inoue K. Prog Polym Sci 2000;25:453.
(e) Voit B. J Polym Sci, Part A: Polym Chem 2000;38:2505.
(f) Hult A, Johansson M, Malmström E. Adv Polym Sci 1999; 143:1.
(g) Hawker CJ. Adv Polym Sci 1999;147:113.
[31] (a) Jansen JFGA, de Brabander-van den Berg EMM, Meijer EW. Science 1994;266:1226.
(b) Jansen JFGA, Meijer EW, de Brabander-van den Berg EMM. J Am Chem Soc 1995;117:4417.
(c) Sunder A, Krämer M, Hanselmann R, Mülhaupt R, Frey H. Angew Chem Int Ed 1999;38:3552.